

## Microphysical Effects of Wintertime Cloud Seeding with Silver Iodide over the Rocky Mountains. Part III: Observations over the Grand Mesa, Colorado

ARLIN B. SUPER AND BRUCE A. BOE\*

*Bureau of Reclamation, Montrose Skywater Office, Montrose, Colorado*

(Manuscript received 6 April 1987, in final form 14 March 1988)

### ABSTRACT

During March 1986, several airborne and ground-based silver iodide (AgI) seeding experiments were conducted over the Grand Mesa, Colorado, during a three-day period of northerly flow and shallow orographic cloud. While little natural snowfall was observed during these experiments, supercooled liquid water formed over the windward slopes and evaporated to the lee of the mesa for many hours. Seeding-induced microphysical changes coincident with the AgI plumes were found in all eight experiments, (including two that employed ground-based seeding) by aircraft sampling about 500 m above the mesa top. Precipitation rates estimated from ice particle images at flight levels suggested increases within the seeded volumes in all but one experiment. Surface precipitation increases were observed in three aircraft seeding experiments and one ground-based seeding experiment that coincided with the passage of AgI plumes aloft. Surface observations were not possible during the other ground-based seeding experiment, but some increase in snowfall is thought probable. Three aircraft seeding experiments failed to show surface snowfall increases, and reasons for this are explored.

### 1. Introduction

The objective of the Colorado River Augmentation Demonstration Program, part of the Bureau of Reclamation's Project Skywater, is to improve cloud seeding technology for the Colorado River Basin. The Grand Mesa of western Colorado was selected as an experimental area particularly well suited for physical investigations of cloud and precipitation responses to the introduction of seeding agents.

Physical cloud seeding experiments were conducted over the Grand Mesa during 18–20 Mar 1986, a period characterized by northerly flow and shallow orographic cloud. The goal of these experiments was to measure directly seeding-induced microphysical changes within cloud and in precipitation at the surface. A more detailed discussion of objectives and the physical hypothesis is given in Part I (Super et al. 1988).

In six experiments, silver iodide (AgI) was produced at varying distances north of the mesa along flight tracks flown approximately perpendicular to the wind. Seeding was conducted at the 3.8 km level (all altitudes msl), the lowest practical flight altitude, which was about 500 m above the mesa top. Subsequent sampling passes by the instrumented aircraft were also flown at 3.8 km, but parallel to the wind, through the seeded zone and over the surface target (hereafter called Snow

Lab, see Fig. 1). The along-the-wind sampling passes continued until the seeded zone passed well downwind of the Snow Lab.

Two other experiments used a ground-based AgI generator on the upwind slope of the mesa. Passes were flown over the top of the mesa and approximately perpendicular to the wind, which allowed sampling of both the seeded cloud volume (hereafter called the "seeding plume" or "seeded zone") and the adjoining natural cloud. Targeting of the Snow Lab was not possible in these cases, and only aircraft measurements were recorded. In one case, cloud base was far enough above the mesa to allow subcloud sampling by the aircraft.

### 2. Project area and operational limitations

The Grand Mesa is a large, flat-topped barrier with an average caprock elevation of between 3.2 and 3.3 km in the study region. It has a vertical rise of about 1.6 km from the floors of the Colorado River Valley to the north, the Grand Valley to the west, and the Uncompahgre Valley to the south. Upper air flow from the north, west and south is unblocked, resulting in a high frequency of orographic storms. The major axis of the mesa is oriented WSW–ENE, so that southerly and northerly flow are especially conducive to the formation of orographic cloud.

An all-weather highway over the mesa top is open year-round, and snowmobiles afford good access to most of the top. Much of the mesa is covered by conifer forest, and clearings provide adequate sites for precipitation gages. Commercial power is available in a few locations on top of the mesa and on the north and

\* Present affiliation: North Dakota Atmospheric Resource Board, Bismark, North Dakota.

Corresponding author address: Dr. Arlin B. Super, Bureau of Reclamation, Code D-3720, Denver Federal Center, Denver, CO 80225.

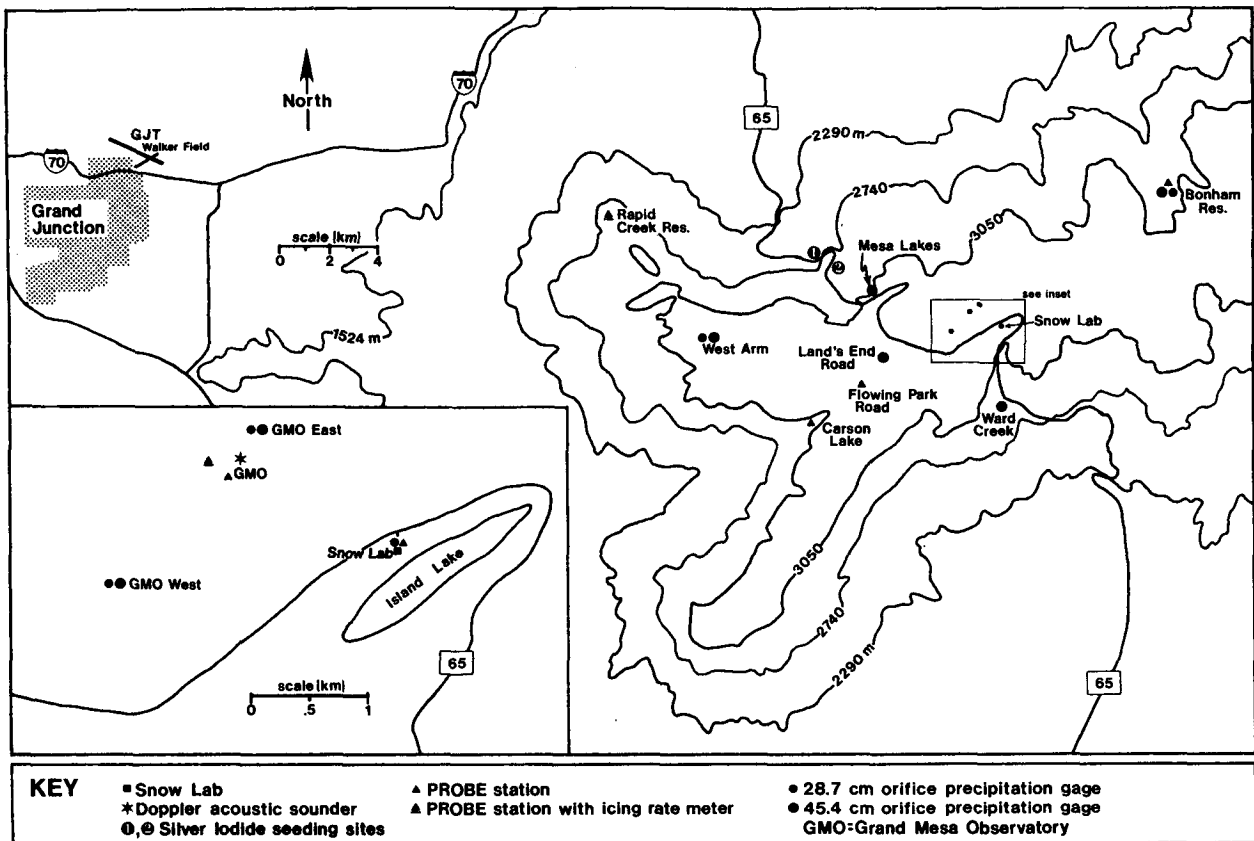


FIG. 1. Map of the Grand Mesa experimental area in western Colorado.

south slopes. Twice daily upper-air soundings are obtained from rawinsondes released by the National Weather Service near Grand Junction, 45 km WNW of the Snow Lab. Because of the absence of higher terrain nearby, a special waiver was obtained from the Federal Aviation Administration (FAA) permitting Instrument Flight Rules (IFR) flight to within 300 m of the highest terrain on the mesa, half the minimum clearance normally required.

The Snow Lab surface target for the seeding experiments was located in a small forest clearing just south of and about 100 m below the southern edge of the mesa caprock, where the wind was typically very light. Instrumentation at the Snow Lab included an ice crystal photography system; other instrumentation locations on the mesa are shown in Fig. 1. The PROBE stations and doppler acoustic sounder provided near-surface and 30–570 m (agl) layer winds, respectively. (A more complete description of the instrumentation and related characteristics can be found in Part I.)

Attempts to detect seeding effects directly had certain operational constraints, for example, the minimum aircraft altitude restriction of 300 m above the highest terrain. This placed the aircraft 500–600 m agl in the area of operations. Thus, a significant layer without

microphysical measurements existed between the lowest aircraft sampling level and the surface. Ice crystals having terminal velocities of  $50 \text{ cm s}^{-1}$  would require about 1000 s to traverse this “layer of uncertainty.” Significant additional growth could occur within this layer if supercooled liquid water (SLW) was present. Particle trajectories might also change markedly within this layer, depending on growth rates and wind shear. The presence of AgI and SLW within this layer was not recorded, although the latter was sometimes detected by tower-mounted icing rate meters at two mesa-top locations (Fig. 1). Sampling by the single research aircraft was done primarily at the 3.8 km level, the altitude of the AgI release. Consequently, the AgI and cloud microphysics were only occasionally monitored at higher levels.

### 3. Ground-based seeding experiments

Experiments were conducted on 19 and 20 Mar to observe by aircraft the ground-released AgI and the associated microphysical effects in the orographic clouds over the Grand Mesa. Flow over western Colorado was northerly, with Grand Junction (GJT) 70 kPa rawinsonde winds ranging from 7 to  $12 \text{ m s}^{-1}$  and 330 to  $010^\circ$  true.

a. Experiment of 19 Mar 1986

The AgI generator was ignited at 1052 (all times MST) at 2.69 km elevation at Site 1 on the north slope (Fig. 1). Silver iodide consumption was  $30 \text{ g h}^{-1}$  until shutdown at 1248 to permit initiation of airborne seeding experiments (see section 4).

An aircraft sounding recorded on climbout near 1130 is shown in Fig. 2c. Stability was neutral through the 60–70 kPa layer of interest. The wind and stability during this and the other physical experiments are discussed in more detail by Holroyd et al. (1988). Tethersonde observations from the seeding site indicated winds in the 2.7–3.2 km layer of  $4\text{--}8 \text{ m s}^{-1}$  from  $315^\circ$  to  $355^\circ$ . Wind directions measured by the doppler acoustic sounder ranged from  $320^\circ$  to  $340^\circ$ , with speeds ranging from 6 to  $7 \text{ m s}^{-1}$  just 50 m above the mesa top and from 9 to  $13 \text{ m s}^{-1}$  at the 3.7 km level. Cloud base during the experiment was just below the mesa top at 3.2 km. Cloud tops were near 4.6 km, capped by a dry stable layer. Digital satellite imagery revealed a fairly uniform cloud deck about 25 km wide covering the entire mesa at the time the seeding began. The southern edge appeared slightly broken.

The first aircraft sampling pass over the mesa was made near 1150. Some cloud tops were penetrated at 4.6 km, where SLW was less than  $0.05 \text{ g m}^{-3}$ , maximum IPC was  $5 \text{ L}^{-1}$ , and air temperature was  $-19.5^\circ\text{C}$ . Ice particles seldom exceeded 0.2 mm and appeared to be compact plates.

Seven crosswind passes followed at 3.8 km altitude, over the Snow Lab and about 6.3 km downwind of the seeding generator. After the fifth pass the aircraft climbed to measure cloud tops, which had risen to 4.9 km and cooled slightly to  $-20^\circ\text{C}$ . Peak SLW amounts had increased to  $0.15 \text{ g m}^{-3}$  at 4.6 km altitude, with IPC in the  $5\text{--}15 \text{ L}^{-1}$  range, again with small, compact ice particles.

All of the first six crosswind passes at 3.8 km altitude detected a zone of enhanced IPC downwind of the AgI generator. The seventh and final pass, made 28 minutes after generator shutdown, detected little AgI, suggesting that most had been transported beyond the sampling line. This is consistent with the tethersonde wind observations.

Total AgI counts recorded during the crosswind passes ranged from 5 (last pass) to 30. The low counts suggest that the 3.8 km sampling level may have been near plume top (Holroyd et al. 1988). The minimum requirement for identification of a plume edge position, 3 counts within 7 seconds (Part I), was achieved on only four passes. These four plume edges were consistent, however, ranging from 7.1 to 8.5 km WSW of the Snow Lab. This position agreed well with the observed wind direction and enhanced IPC zone.

With rare exceptions, the IPC exceeded  $10 \text{ L}^{-1}$  only from 5 to 9 km WSW of the Snow Lab. The edges of the seeding-enhanced IPC zone (hereafter "seeded

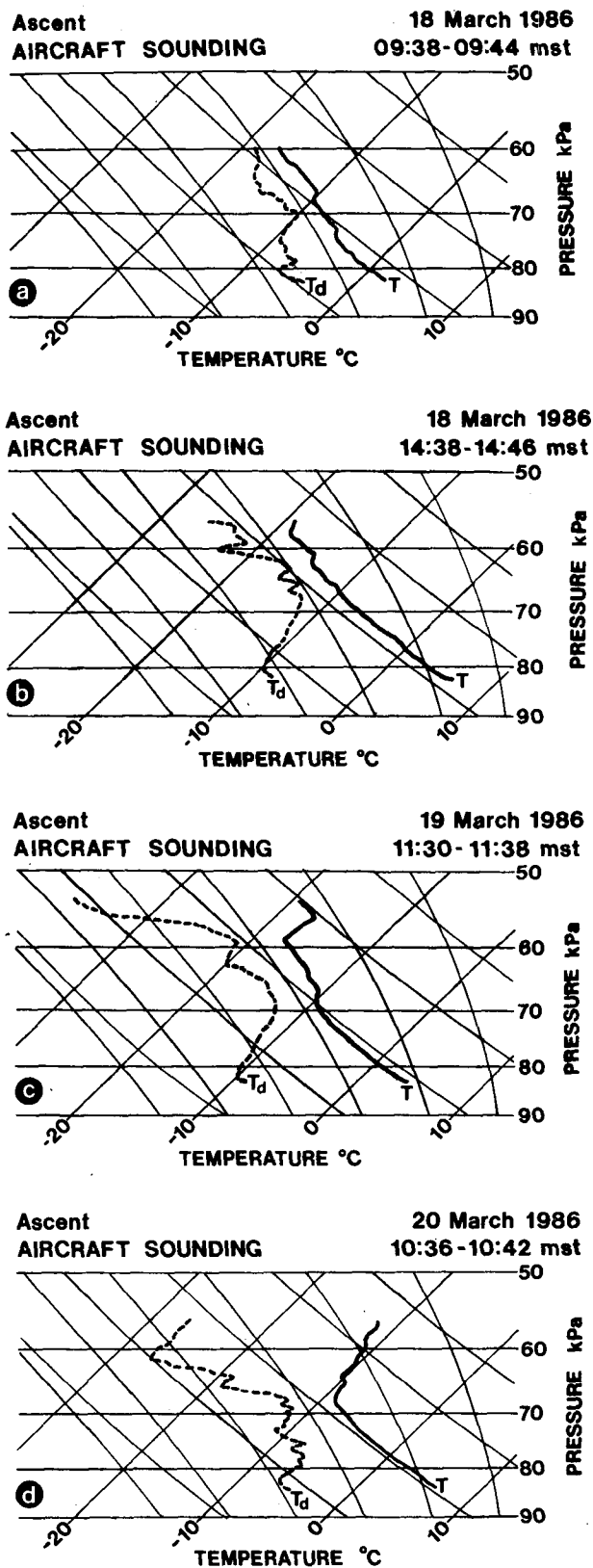


FIG. 2. Temperature and dewpoint temperature profiles recorded by aircraft during the three-day experimental period.

TABLE 1. Summary of seeded zone for 3.8 km passes with ground generator on 19 Mar 1986.

Pass	Time of seeded zone penetration (MST)	Seeded zone edge positions* (WSW from Snow Lab) (km)	Seeded zone center* (km)	Seeded zone width (km)	Maximum IPC ( $L^{-1}$ )	Mean IPC ( $L^{-1}$ )	Volume sampled (L)	Total acoustical counter counts
1	1200	5.27-5.86	5.6	0.6	48	17	13.6	11
2	1209	5.80-8.41	7.1	2.6	74	16	56.0	28
3	1221	6.76-8.09	7.4	1.3	101	21	25.1	30
4	1230	7.37	7.4	<0.1	94	82	0.4	22
5	1240	6.11	6.1	<0.1	22	22	1.1	7
6	1309	6.13-6.89	6.5	0.8	120	50	8.3	21
7	1316	5.0 -9.0**	—	—	4	2	149.0	5

\* WSW from Snow Lab.

\*\* Approximate zone based on earlier passes (AgI generator off at 1248).

zone”) were thus defined for each pass according to where the IPC fell below  $10 L^{-1}$  and remained below that level for at least a few kilometers beyond. Seeded zone information is summarized for each pass in Table 1. In general, the seeded zone was quite narrow at 3.8 km altitude, exceeding 1.0 km on two passes but less than 0.1 km on two others. A 0.5 km plume width measured at the aircraft sampling line 6.3 km down-

wind of the AgI generator corresponds to only  $4.5^\circ$  of arc. Mean seeded zone IPCs ranged from 16 to  $50 L^{-1}$ , except for the very narrow plume recorded on pass 4 and the low postseeding concentration observed on pass 7. As will be shown, the natural mean IPC was near  $3 L^{-1}$ .

The high-resolution precipitation gage network recorded at most only intermittent trace amounts during

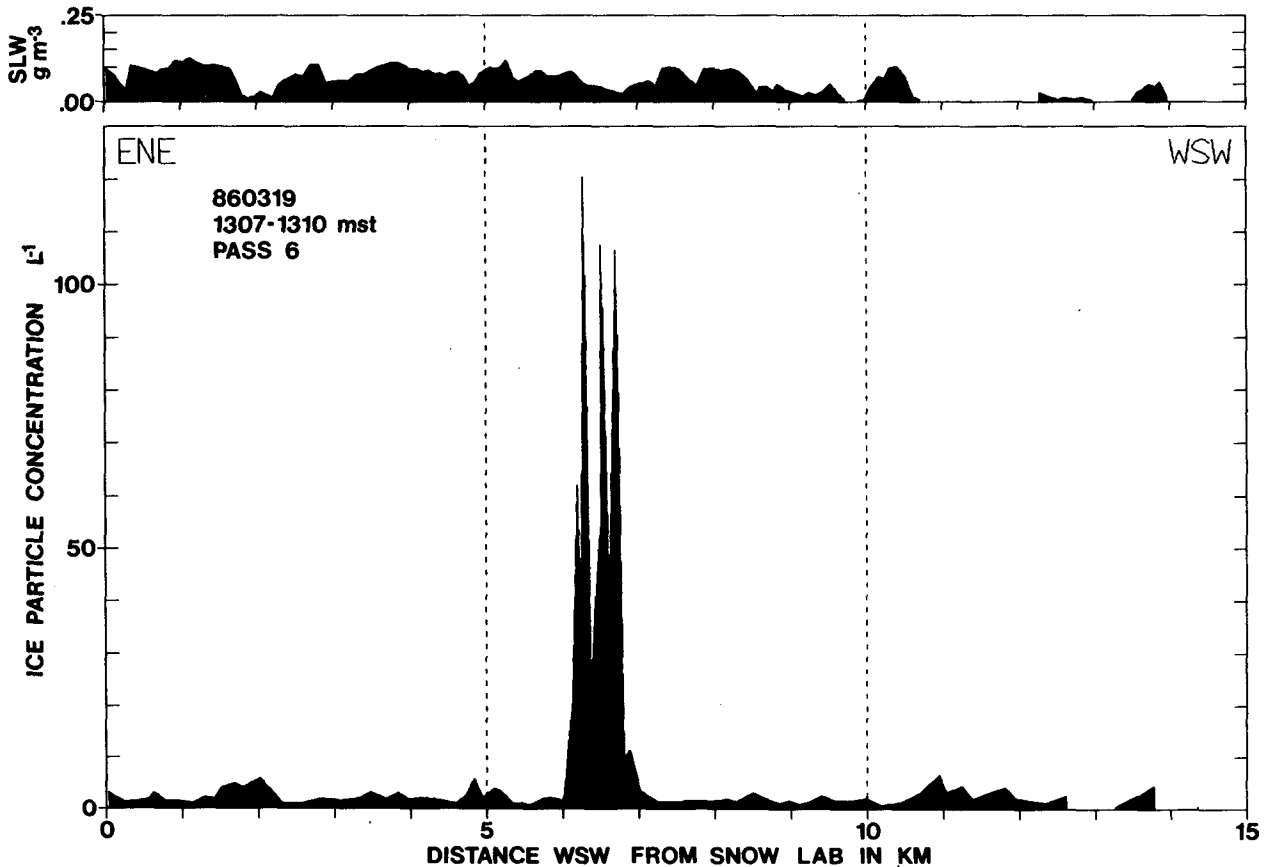


FIG. 3. Buffer-by-buffer ice particle concentration and supercooled liquid water content recorded on 19 Mar during the first ground-based seeding experiment.

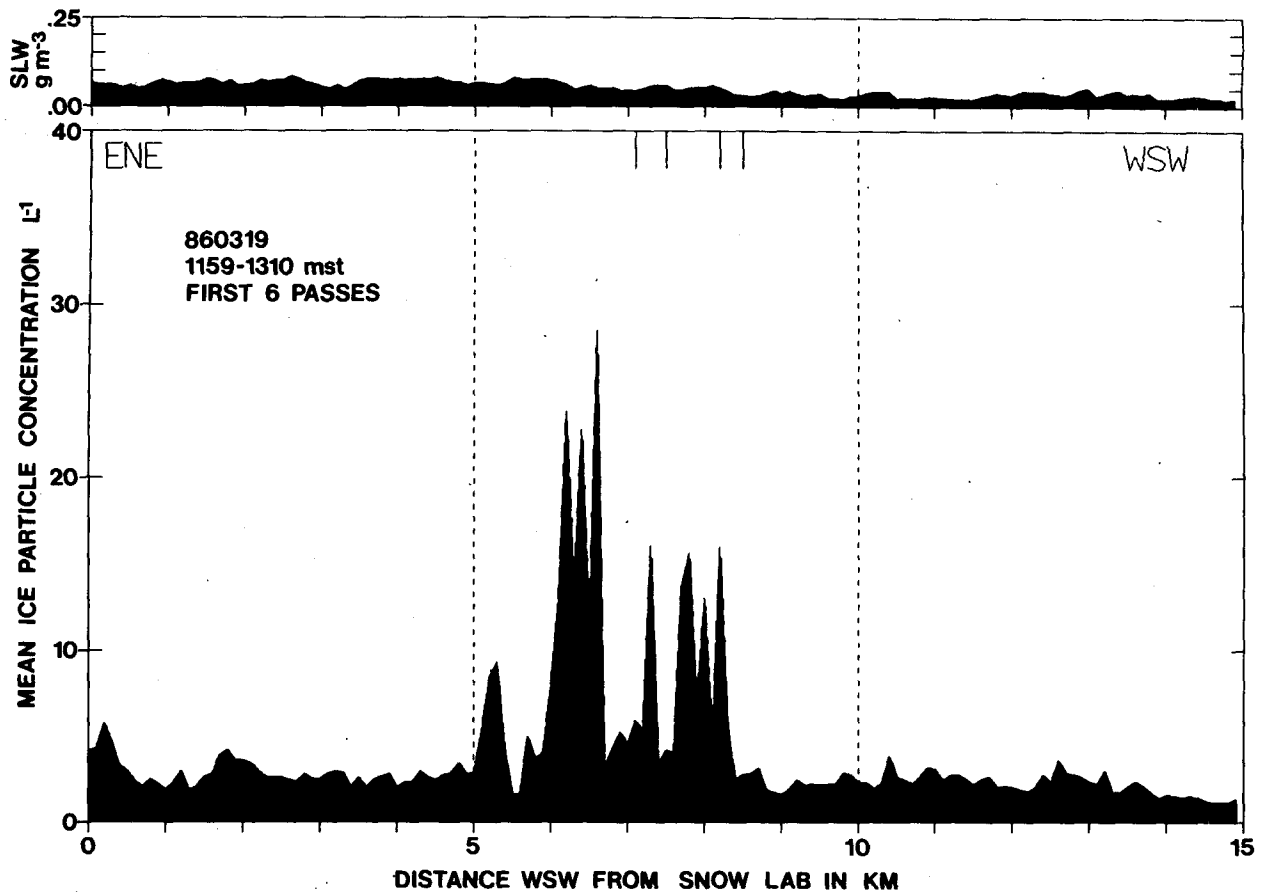


FIG. 4. Mean IPCs and SLW contents recorded on six crosswind passes through the seeding plume during the ground-based seeding experiment of 19 Mar 1986. AgI plume edges are noted by vertical lines at the top of the IPC plot.

the experiment. No precipitation gages were located under the seeded zone, and the closest crosswind gage recorded no snowfall.

Figure 3 shows buffer-by-buffer IPC (discussed in Part I) and 1 Hz SLW observations for the sixth pass at 3.8 km. The width of the seeded zone is 0.8 km, near the median of the seven passes. The fine-scale structure in the essentially instantaneous sample is well illustrated. No definite SLW reduction was observed in association with the seeded zone on this or the other six passes, though there was some suggestion of it.

The mean IPC and SLW for the first six 3.8 km passes are shown on Fig. 4, along with the AgI plume edge positions estimated for the four passes having sufficient ice nucleus counts. In general, less SLW was observed to the WSW. The seeded zone is quite evident, but it meandered over 3.2 km (from 5.1 to 8.3 km WSW of the Snow Lab) during the course of the experiment.

Comparison of the microphysical characteristics within the seeded zone with those of nearby natural cloud was accomplished by defining 2 km-wide crosswind control zones to the ENE and WSW of the seeded zone. One km-wide buffer zones separated the seeded

and control zones. Ice particle sizes, concentrations and habits were calculated for each zone and pass by the method in Holroyd (1987). The means for each seeded, buffer and control zone for passes 1, 2, 3 and 6 are shown in Fig. 5. (Passes 4 and 5 were excluded due to their extremely narrow plume widths and low AgI counts, which suggests that they were nearer to plume top than the other passes.) Ice particle concentrations of about  $3 \text{ L}^{-1}$  were found in the control zones (ENEC, WSWC) and buffer zones (ENEB, WSWB), while IPC averaged  $26 \text{ L}^{-1}$  in the seeded zone (SZ). Most of the increases arose from ice particles with a maximum dimension of less than 1 mm. (Note: The length limits were chosen to provide a logarithmic scale;  $\log 0.10 = -1.0$ ,  $\log 0.16 = -0.8$ ,  $\log 0.25 = -0.6$ , etc.) Most ice particles within the seeded zone were classified as spherical, hexagonal or irregular, with a lesser increase in dendritic crystals. The mean temperature at the sampling level was  $-14^\circ\text{C}$ , so that dendritic crystals would be expected with SLW present (Magono and Lee 1966).

The sampling line was only 6.3 km downwind of the generator, and the generator itself was not in cloud. The aircraft-measured wind speed was  $14 \text{ m s}^{-1}$  over

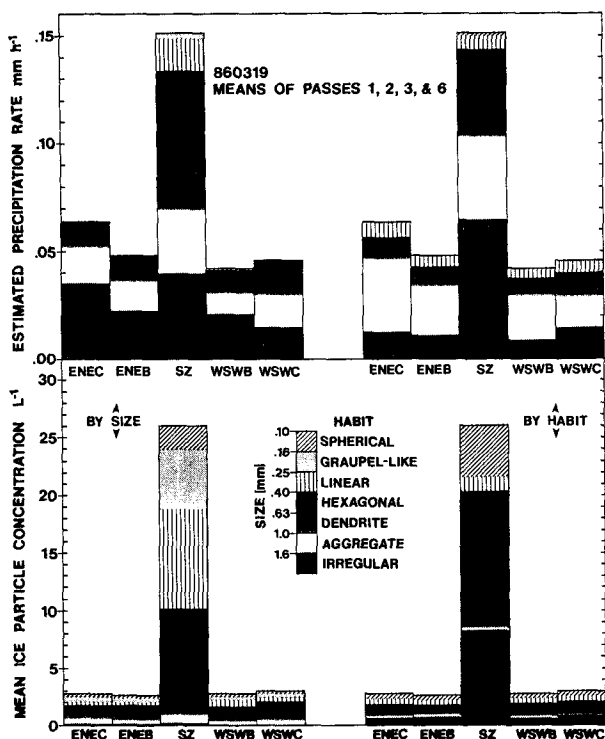


FIG. 5. Mean IPCs and estimated precipitation rates recorded by aircraft at 3.8 km msl in the seeded and nonseeded zones during the ground-based seeding experiment of 19 Mar 1986. The particle size/habit shadings apply to both top and bottom panels. See text for zone identifiers.

the mesa top at 3.8 km, while speeds near the mesa surface were 6–7 m s<sup>-1</sup>. Assuming a mean wind speed in the layer below the aircraft sampling level of 10 m s<sup>-1</sup> and a mean in-cloud distance of the plume upwind of the sampling line of 5 km, cloud passing the sampling line would have been subjected to the effects of the AgI for about 500 s. Since contact nucleation was presumably the ice-forming mechanism for the AgI-NH<sub>4</sub>I smoke (DeMott et al. 1983), crystal formation would have been a continuous process, which could explain the range of sizes found in the seeded zone. Observations by Holroyd (1986) showed that crystal growth rates near 0.1 mm min<sup>-1</sup> were appropriate at -14°C in shallow orographic clouds over the mesa. Therefore, crystals of about 1 mm would be the largest expected from the AgI seeding, which is consistent with Fig. 5.

When visually examined, many of the small 2D-C images classified as spherical, hexagonal or irregular appeared to be embryonic dendrites with limited branching. Given more growth time these crystals probably would have been classified as dendrites by Holroyd's software. In addition, some small crystals appeared to be joined with larger (presumably natural) dendrites, suggesting the beginnings of aggregation.

Precipitation rates estimated from 2D-C images using Holroyd's (1987) scheme are also shown in Fig. 5

according to crystal habits and sizes. All precipitation (or snowfall) rates, whether at aircraft levels or on the surface, are given as melted water equivalents. These estimated precipitation rates should be interpreted only in a qualitative sense due the limitations discussed in Part I. Within the seeded zone, the precipitation rate approximately tripled, largely because of increases in the number of crystals smaller than 1 mm and mostly classified as irregular or aggregates, with lesser increases in dendritic and hexagonal crystals.

#### b. Experiment of 20 Mar 1986

Northerly flow persisted for the third consecutive day. A shallow stratocumulus deck lay over the Grand Mesa during the morning hours, capped by a dry, stable layer (Fig. 2d). Cloud conditions initially seemed unsuitable for physical experiments, so an AgI plume tracing mission was undertaken.

The seeding generator was ignited at Site 1 on the north slope at 1025. At 1055 highest cloud tops over the mesa were measured by the aircraft at 4.3 km and -12.5°C, but most of the ragged, broken deck lay below 4.1 km and contained little SLW. Cloud bases were near 3.6 km, high enough to permit Visual Flight Rules (VFR) sampling of the AgI plume below cloud base. Visible satellite imagery at 1030 indicated that the orographic cloud was about 18 km wide.

Several crosswind passes were made at differing altitudes, defining the vertical and horizontal extents of the AgI plume 5.5 km downwind of the seeding generator. The generator was subsequently turned off at 1225, moved to Site 2, also on the northern slope but 220 m higher (Fig. 1), and reignited at 1251 to determine what modifications in the plume might result from the higher site.

While the seeding generator was being moved, the aircraft crew realized that the position of the seeding plume coincided with that of a weak snow shower first observed south of the seeding line at 1148. No snowfall had been visible below cloud base at 1131 when bases were near 3.65 km. Visibility over the mesa top was at least 60 km for the duration of the mission, yet no other snowfall was observed except downwind of the generator and south of the initial sampling line.

Four IFR passes were made at the 3.8 km level between 1251 and 1319, three crosswind and one along-the-wind. All encountered IPCs exceeding 50 L<sup>-1</sup>. Total counts from the acoustical counter ranged from 132 to 262 per pass. Estimated AgI plume edges were in close agreement with the ice particle plumes, which were several kilometers wide on each crosswind pass. The natural (nonseeded) IPC was observed to be almost zero. During these passes clouds were less than 500 m thick, and tops were no colder than -12°C.

Winds recorded by the doppler acoustic sounder between 1245 and 1500 ranged from 345 to 010° and 3.0 to 5.5 m s<sup>-1</sup> near the surface, to 350 to 035° and

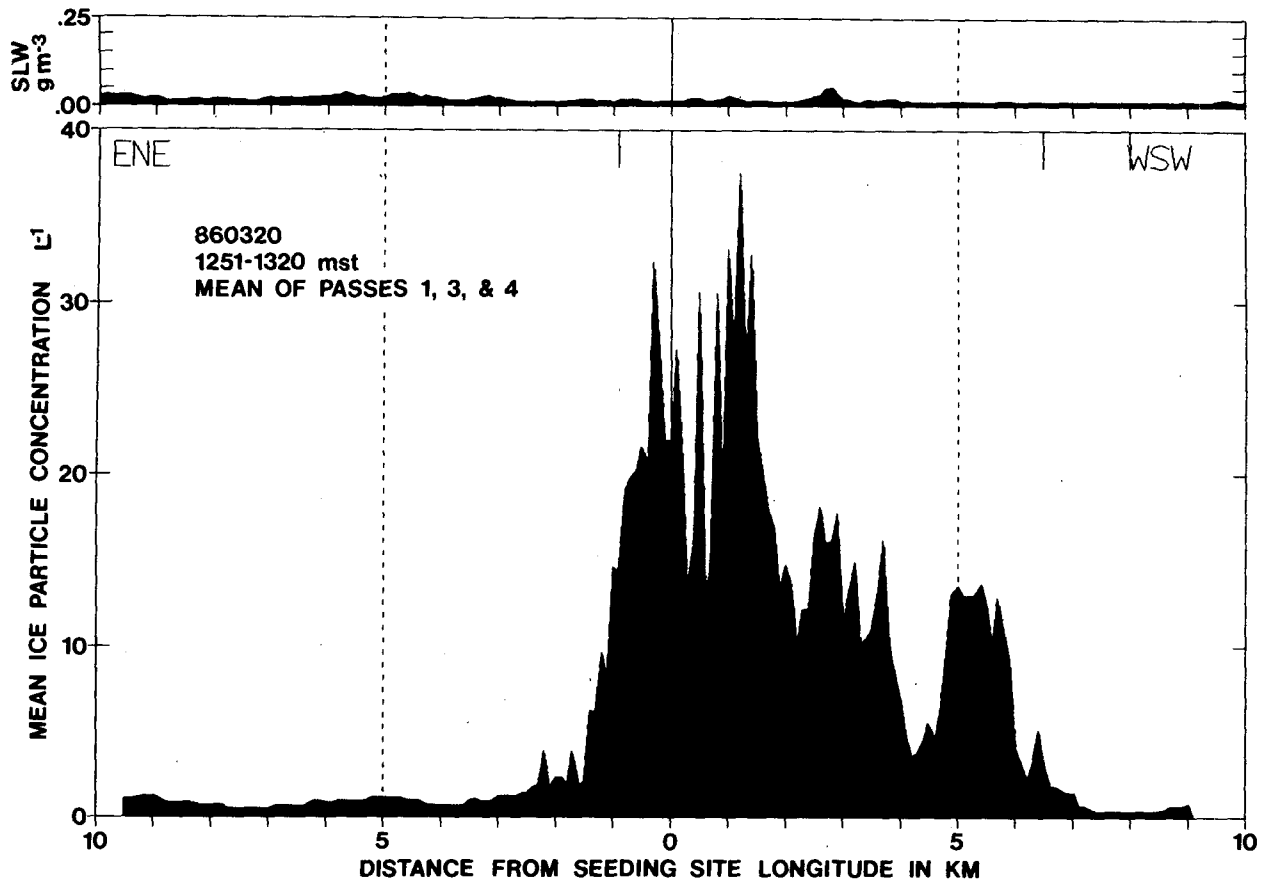


FIG. 6. As in Fig. 4 for three crosswind passes during the ground-based seeding experiment of 20 Mar 1986.

4.0 to 7.0  $\text{m s}^{-1}$  near the 3.8 km aircraft sampling level. With these speeds, AgI transport times to the sampling line about 11 km downwind of the generator would have been between 0.5 and 1.0 h. Thus, AgI released until 1225 from Site 1 might have affected the cloud as late as 1325, but AgI from Site 2, first produced at 1251, should have been at or near the sampling line by that time. No decreases in IPC or plume widths were apparent in the three crosswind passes between 1251 and 1319.

Figure 6 shows the mean IPC, SLW content, and AgI plume edge positions observed on the three crosswind passes made near 11 km from the AgI generator (referenced to the seeding site longitude). Peak SLW values on the individual passes (not shown) were near  $0.05 \text{ g m}^{-3}$ . The width of the enhanced IPC zone ranged from 7 to 8 km on the individual passes with boundaries meandering only over 1 to 2 km. The plume width was obviously much greater than on the previous day.

An analogous plot for the single pass parallel to the wind (Fig. 7) revealed peak SLW contents near  $0.1 \text{ g m}^{-1}$  from above the seeding site to 7 km downwind of it. Ice particle concentrations in excess of  $100 \text{ L}^{-1}$  were found coincident with the leading edge of the AgI plume. A secondary maximum was found about 15

km south of the seeding site, which rapidly decreased further south in leeward subsidence.

The edges of the seeded zones for the 3.8 km crosswind passes were defined by IPC exceeding  $2 \text{ L}^{-1}$ , and the seeded zones thus defined subdivided into thirds. Control zones 3 km wide were established beyond buffer zones of 0.1 km width. Mean concentrations in the seeded zones ranged from 9 to  $16 \text{ L}^{-1}$ , and the estimated precipitation rate reached  $0.11 \text{ mm h}^{-1}$ , compared with essentially nil precipitation in the controls. Crystals in the seeded zones were again predominantly hexagonal and less than 0.6 mm in size, yet larger particles contributed two-thirds of the precipitation.

At 1331, a final crosswind pass was made through the precipitation shaft of the visibly dissipating shower at the 3.25 km altitude (150 m agl). The precipitation shaft was 2 km wide and 15 km SSW of the seeding site at that time, and a new shower could be seen to the north. The mean IPC was  $6 \text{ L}^{-1}$  and the estimated precipitation rate near  $0.04 \text{ mm h}^{-1}$ . The acoustical ice nucleus counter registered 128 counts.

The second shower was also sampled in cloud and below cloud base. The AgI plume edges were again coincident with the beginnings of the enhanced IPC

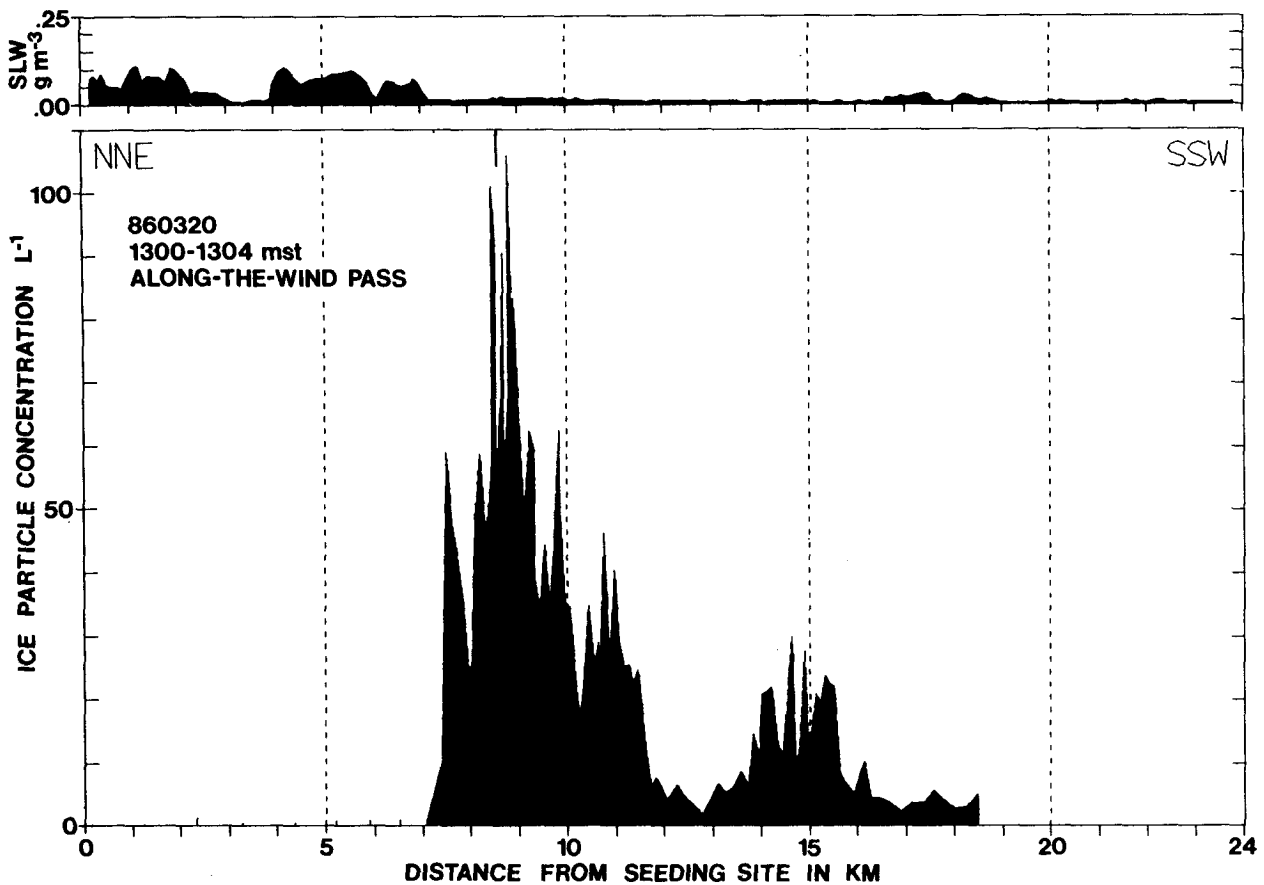


FIG. 7. As in Fig. 4 for a single pass flown along-the-wind during the ground-based seeding experiment of 20 Mar 1986.

zones. The mean IPC in the central seeded zone at 3.25 km (below cloud) was  $19 \text{ L}^{-1}$ , with an estimated precipitation rate of  $0.14 \text{ mm h}^{-1}$ . The snowfall was again visually observed to be reaching the surface. The crosswind control zones had  $1 \text{ L}^{-1}$  IPC and essentially zero snowfall rate.

A third shower developed only 8 km south of the seeding generator after the second shower began to dissipate in the lee of the mesa. Crosswind sampling in cloud and below base yielded results very similar to the earlier showers: The central seeded zone IPC at 3.45 km altitude was  $26 \text{ L}^{-1}$  with an associated precipitation rate of  $0.11 \text{ mm h}^{-1}$ . The mean IPC was well below  $1 \text{ L}^{-1}$ , and precipitation rates were again virtually zero in the adjoining nonseeded zones.

Five final passes at 3.8–3.85 km altitude both crosswind and parallel with the wind again found SLW contents up to  $0.1 \text{ g m}^{-3}$  above the windward slope. Peak IPCs observed on these passes, nearer the AgI generator, increased to 40–100  $\text{L}^{-1}$ , coincident with pass-total counts up to 414 from the acoustical counter.

#### c. Summary of ground-based seeding experiments

Silver iodide released from either 285 or 505 m below the top of the Grand Mesa was consistently transported

well above the mesa top within several km downwind of the generator. The AgI plume was quite narrow on 19 Mar and quite wide on 20 Mar, in agreement with the observed differences in horizontal wind fluctuations. Holroyd et al. (1988) discuss in detail the plume, wind and stability characteristics for these and several other experiments with ground-released AgI.

Seeding produced dramatic enhancements in IPC, mostly crystals smaller than 0.6 mm. Many of these were embryonic dendrites on 19 Mar when the temperature at the sampling level was  $-14^\circ\text{C}$ , but were hexagonal on 20 Mar when the temperature of the shallow stratocumulus deck was between  $-8.5$  and  $-11.5^\circ\text{C}$ .

Estimated precipitation rates within the seeded zones at 3.8 km altitude were near  $0.1 \text{ mm h}^{-1}$  on both dates. This was about triple the natural rate on 19 Mar, while natural precipitation was virtually nil on 20 Mar. (Note: these calculated precipitation rates are believed to be underestimates, and caution should be used in quantitative interpretation.)

#### 4. Airborne seeding experiments

Six similar direct detection cloud seeding experiments were conducted on 18 and 19 Mar 1986. In each

experiment a single airborne line of AgI was released approximately perpendicular to the wind at a constant distance upwind of the Snow Lab at 3.8 km altitude.

After each seeding arc was completed, a series of passes was flown over the Snow Lab and parallel to the wind at the 3.8 km level. These passes were intended to monitor the evolution of the AgI plume and the resulting cloud microphysical changes during transport over the mesa. Surface observations of snowfall characteristics were made at the Snow Lab during each experiment, primarily with the ice crystal photography system (see Part I). In addition, high resolution weighing precipitation gages with 45.4 cm orifices and Alter-II shields were operated in protected clearings at seven sites (Fig. 1). The gage charts were read each 15 minutes to the nearest 0.025 mm with the aid of magnification.

The seeded zones in these airborne experiments were defined for each pass parallel to the wind according to marked increases in IPC above the general background and/or the presence of AgI as detected by the acoustical

counter. The presence of AgI was at times observed exclusive of IPC in regions devoid of SLW, while IPC was occasionally observed without AgI, probably due to scavenging and/or transport of the AgI plume to levels above or below that of the aircraft.

The following criteria were used in determining seeded and nonseeded zones: 1) regions containing the AgI plume were considered seeded; 2) regions having an IPC significantly above the preseeding natural concentrations observed over the mesa were considered seeded if associated with an AgI plume; and 3) regions having an IPC significantly above natural concentrations were also considered seeded in the absence of an AgI plume if consistent in position with the advection of a volume previously defined as seeded. The nonseeded or natural (control) cloud was considered to be cloud volume free from any effects of AgI, including the possibility of contamination from aloft resulting from speed shear of the horizontal wind. Figure 8 shows the relative ease with which approximate plume

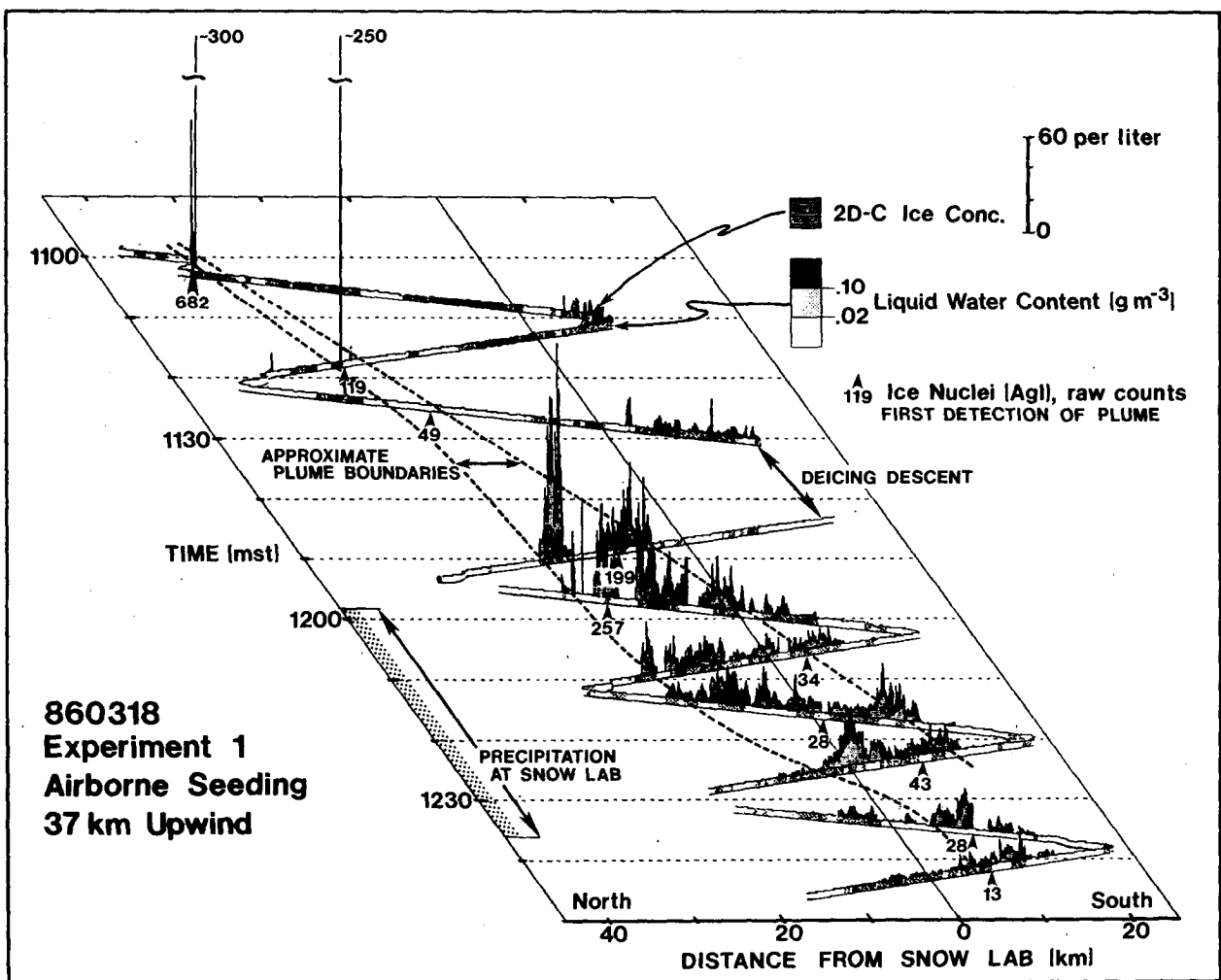


FIG. 8. Ice particle concentrations and SLW content plotted as functions of time and distance from the Snow Lab target for the first airborne seeding experiment. Also shown are the pass-total ice nucleus counts and the estimated locations of the AgI plume edges.

boundaries can be defined. Those portions of cloud not clearly either seeded or nonseeded were excluded from further evaluation. The 5 km interval upwind of the Snow Lab was evaluated separately for the seeded and nonseeded classifications to determine the microphysical differences.

Although the first airborne seeding experiment was no more successful than some of the others, it is discussed in some detail. In the interest of brevity, however, only the essential points of the other five similar experiments are presented. Section 4g summarizes the results of all airborne seeding experiments and presents supporting information for each.

#### a. Airborne seeding experiment 1

At 0500 on 18 Mar 1986 a deep trough lay over the Rocky Mountain states. At 50 kPa the trough axis ran from El Paso, Texas, over the Oklahoma Panhandle, across central Nebraska, and northward to Bismarck, North Dakota. A strong short-wave trough had passed through southern Arizona and New Mexico in the previous 12 hours.

The GMO tower-mounted icing rate detector (Fig. 1) indicated continuous SLW in the orographic stratocumulus cloud at 70 m above the mesa top from 1600 on 17 Mar until 1300 on 18 Mar. Thereafter near-surface SLW was observed between 1900–2100 on 18 Mar but not at all during the experiments on 19 Mar. Flow was northerly after the passage of the long-wave trough.

Three pretreatment passes were flown between 1013 and 1041 on 18 Mar, parallel with the winds (essentially on a north–south axis) at 3.8 km altitude, where the temperature was  $-14^{\circ}\text{C}$ . These passes detected maximum SLW content of  $0.15\text{ g m}^{-3}$  and essentially no ice except 5–10 km south of the Snow Lab, where the mean IPC was less than  $2\text{ L}^{-1}$ . Highest cloud tops were 4.0 km and  $-15.5^{\circ}\text{C}$ , while bases were near the surface (3.2 km). The aircraft sounding recorded on climbout from Montrose (Fig. 2a) revealed slight instability from just below 71 kPa up to about 68 kPa.

The first seeding arc on 18 Mar was generated near 1057 at 3.8 km altitude and about 37 km upwind of the Snow Lab target. Satellite imagery at 1100 revealed solid orographic cloud for some 20 km upwind of the Snow Lab, with broken clouds extending about another 10 km farther north. This proved to be the greatest upwind cloud coverage observed during any of the experiments.

Ten postseeding passes parallel with the wind documented the plume and cloud evolution (Fig. 8). On the first three passes, the seeded zone was marked by the presence of AgI and twice by very high IPC in quite narrow zones. Natural ice remained limited to the area 5–15 km downwind of the Snow Lab. Airframe icing necessitated a descent to deice after the third pass.

A considerably broader ice crystal plume was en-

countered coincident with AgI on the fourth pass, about 1150. Twenty-two minutes had elapsed since the seeded volume had last been sampled and the AgI had entered the continuous orographic cloud deck.

Aircraft winds recorded along each north–south pass over the mesa were examined to determine the accelerations induced by the barrier in the northerly flow. For the three flights on 18–19 Mar, the mean wind speed at the 3.8 km aircraft altitude was  $8\text{--}10\text{ m s}^{-1}$ . Wind decelerations were consistently recorded from about 20 to 10 km upwind of the Snow Lab, followed by accelerating flow from 10 km upwind to overhead of the Snow Lab. The speed minimum of around  $7\text{ m s}^{-1}$  was consistently found about 10–15 km upwind of the Snow Lab, while the maximum speed of  $13\text{--}15\text{ m s}^{-1}$  was invariably found over or within a few kilometers upwind of the Snow Lab. The accelerating flow presumably stretched the seeding plume as it crossed the Mesa. It is likely that the enlargement of the seeded volume was further aided by turbulent mixing and vertical wind shear within the stratocumulus cloud.

The seeded zone continued to broaden as it passed over the mesa (passes 5, 6, 7). Observed IPC gradually began to decrease, and AgI counts diminished sharply, probably due to the combined effects of turbulent mixing, diffusion, nucleation, and scavenging of the AgI by cloud droplets and ice particles.

The final three passes (8, 9, 10) showed diminishing IPC, most likely resulting from both precipitation and leeside subsidence and sublimation. Little ice or SLW was detected farther than 15 km south of the Snow Lab because the aircraft was generally out of cloud.

The mean IPCs recorded within seeded and nonseeded cloud in the 5 km immediately upwind of the Snow Lab throughout the duration of the experiment are shown in Fig. 9. The mean IPC in the seeded cloud volume was  $6.6\text{ L}^{-1}$ , compared to less than  $1\text{ L}^{-1}$  in the nonseeded cloud. Most of the increase was attributed to small crystals, classified as hexagonal and spherical, whose images often appeared to be embryonic dendrites too small to be adequately classified by the software.

The mean estimated precipitation rate in the seeded zone was  $0.16\text{ mm h}^{-1}$ , greatly exceeding the  $0.01\text{ mm h}^{-1}$  recorded in the nonseeded zone. The increase was largely attributable to crystals classified as aggregates (mostly of dendrites), as well as irregular particles, large numbers of smaller hexagonal crystals, and a trace of graupel-like snow. The importance of aggregation in the lower regions of winter orographic clouds has recently been demonstrated by Cotton et al. (1986). Most of the observed IPC enhancement appeared as crystals less than 0.6 mm in diameter, while most of the estimated precipitation rate in the seeded zone was attributable to crystals 1.0 mm or larger.

Surface snowfall rates were derived from Snow Lab ice crystal photographs in the following manner: Chilled glass collection plates were exposed to snowfall

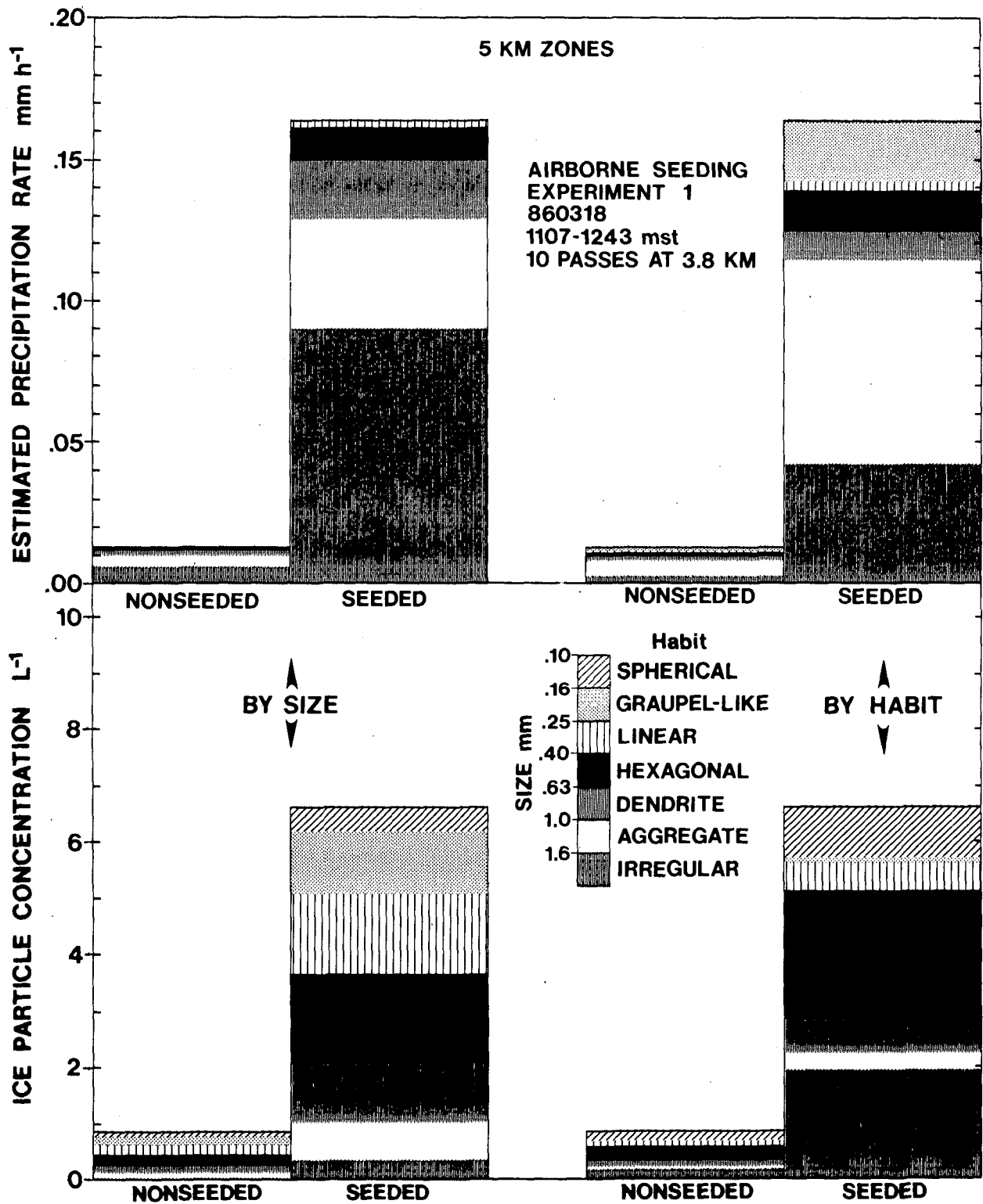


FIG. 9. Mean IPCs and estimated precipitation rates within 5 km upwind of the Snow Lab by crystal habit and size for seeded and nonseeded periods during the first airborne seeding experiment.

for recorded intervals, and the same  $4.7 \times 7.1$  cm area of each sample was photographed. Deliberately photographing the same area of every sampling plate eliminated the possibility that the camera operator might select the largest or most interesting crystals as subjects. The 35 mm negatives were projected at a magnification of 13.5, and each crystal visually evaluated according to size and habit. The size bins employed were the same as those used for evaluation of the aircraft 2D-C probe images. Crystals were classified as either dendrite, aggregate, graupel-like, hexagonal (compact), or irregular. Holroyd's (1987) spherical category was included with the hexagonal category in the photography evaluations. Most of the crystals in the former were smaller than about 0.4 mm, too small to classify more precisely. The typical photograph contained images of 230 ice particles collected over a 30 s interval. The average sample volume per photograph was approximately 15 L.

Precipitation began at the Snow Lab at 1158 and continued at rates up to  $1.1 \text{ mm h}^{-1}$  until 1237 (Fig. 10). Most of the crystals were classified as hexagonal (plates) or irregular, the latter largely being fragments

of dendrites. Most of the precipitation mass was comprised of dendrites between 0.6 and 1.0 mm, aggregates (of dendrites) up to 10 mm, irregular crystals, and even some heavily rimed graupel-like snow. The period of precipitation coincided with the passage of the seeded zone over the Snow Lab (see Figs. 8, 11). Virtually no snowfall was recorded within 0.5 h before or after the passage of the seeded zone. Precipitation amounts upwind of the Snow Lab ranged from 0.025 mm at the Land's End gage site (between 1145 and 1200) to 0.150 mm at the GMO East and GMO West gages (between 1200 and 1245), coincident with the passage of the seeded zone. The mechanical gages are known to respond for some minutes after the cessation of precipitation. No gage indicated precipitation after 1300, and none at all was recorded at Ward Creek, the only site downwind (and downslope) of the Snow Lab.

*b. Airborne seeding experiment 2*

The second arc of AgI was generated 19 km upwind of the Snow Lab, half the distance of the first. When seeding was completed at 1252, the orographic cloud

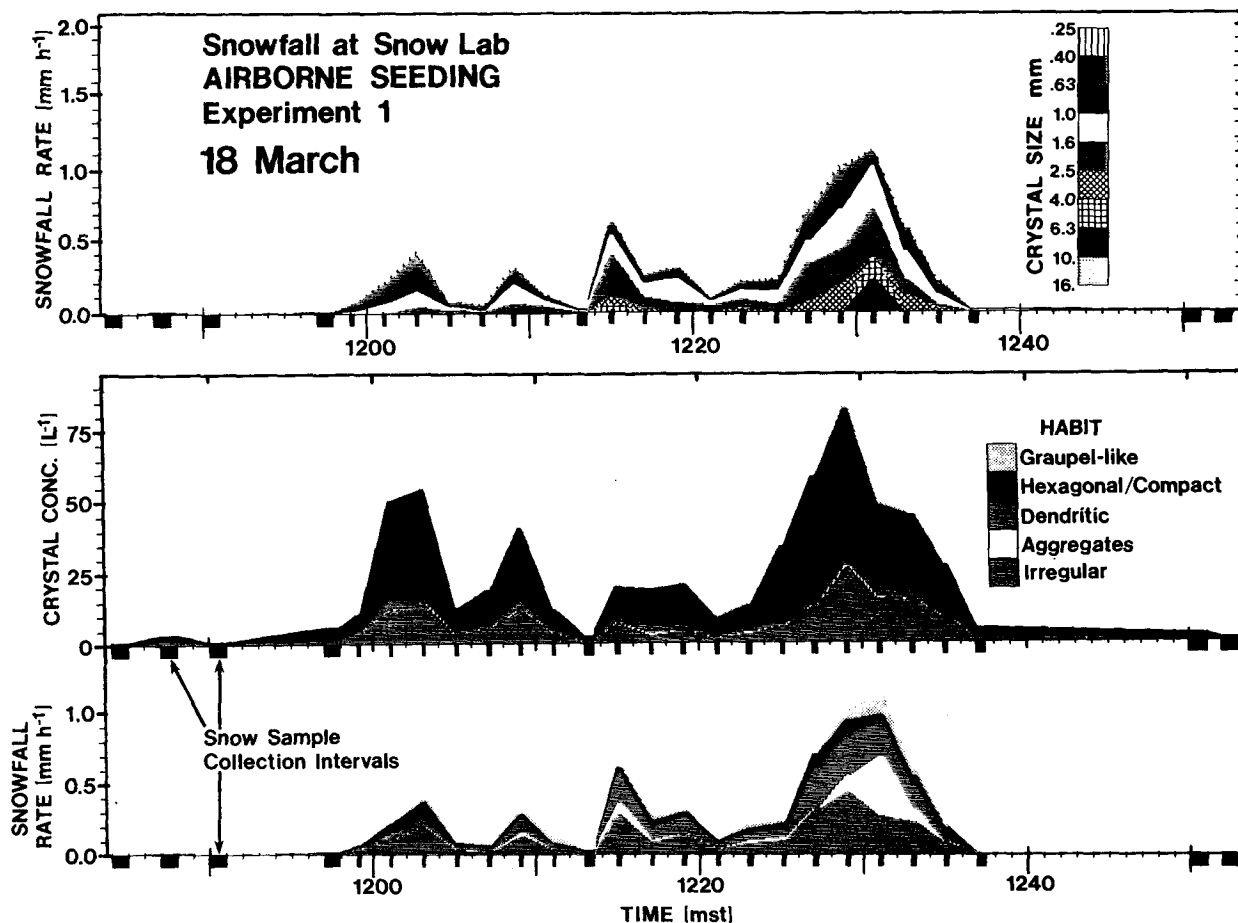


FIG. 10. Characteristics of the snowfall recorded at the Snow Lab by photography of sedimentation slides for the duration of the first airborne seeding experiment. Sampling intervals are shown by the black rectangles along the abscissa.

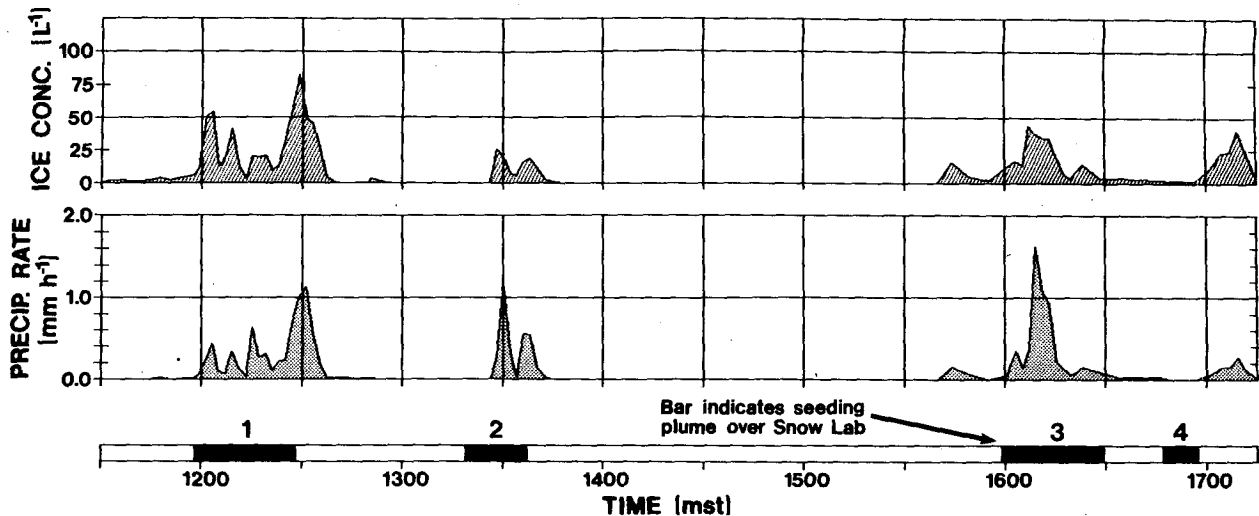


FIG. 11. Precipitation rates and IPCs recorded by photography at the Snow Lab during the four airborne seeding experiments of 18 Mar 1986 compared with a time bar indicating the passage of the seeded zone aloft.

deck extended between 10 and 15 km upwind of the Snow Lab, with scattered cloud over the valley to the north. The cloud deck over the mesa contained SLW up to  $0.2 \text{ g m}^{-3}$  but little ice, and the coldest cloud tops were warmer than  $-16^\circ\text{C}$ .

Total AgI counts per pass ranged from 97 to 358 on the six postseeding passes. A maximum IPC between 40 and  $100 \text{ L}^{-1}$  was encountered coincident with the AgI plume on each pass after the AgI entered the orographic cloud. Nonseeded cloud south of the Snow Lab, however, still contained very little ice. Only limited SLW was found in the core of the seeded cloud on either of the final two passes. The mean IPCs in the 5 km upwind of the Snow Lab in the seeded and nonseeded clouds were  $21 \text{ L}^{-1}$  and  $0.2 \text{ L}^{-1}$ , respectively. The enhancement was again identified by the processing software as predominately consisting of small hexagonal plates. Calculated precipitation rates in the 5 km-wide zone upwind of the Snow Lab averaged  $0.40 \text{ mm h}^{-1}$  when seeded and  $<0.01 \text{ mm h}^{-1}$  when nonseeded.

The seeded zone passed over the Snow Lab between 1319 and 1337, while precipitation began there at 1327 and lasted until 1341 (Fig. 11). As observed in airborne experiment 1, the higher surface precipitation rates resulted largely from aggregates and dendrites. The GMO West high resolution precipitation gage recorded 0.025 mm, the minimum resolvable, between 1330 and 1345. The other gages detected no precipitation during this experiment.

### c. Airborne seeding experiment 3

After landing and refueling, the aircraft returned to the Grand Mesa at 1454. The stratocumulus cloud tops had risen and cooled slightly, to 4.6 km and  $-18^\circ\text{C}$ ,

and the orographic cloud deck extended 15 km upwind of the Snow Lab. The cloud base was still near the mesa top, as indicated by the GMO icing rate detector. The ascent sounding is shown in Fig. 2b. Peak SLW contents of  $0.2 \text{ g m}^{-3}$  were observed a few kilometers north of the Snow Lab.

The third seeding arc was completed at 1509, 28 km upwind of the Snow Lab. Strong AgI signatures were detected in clear air on each of the first four sampling passes and in concert with high IPCs on each of the last six passes, after the AgI entered the cloud. Within the 5 km zone upwind of the Snow Lab, mean IPCs were  $13 \text{ L}^{-1}$  when seeded, compared to  $2 \text{ L}^{-1}$  when nonseeded. Calculated precipitation rates were  $0.34 \text{ mm h}^{-1}$  when seeded and  $0.08 \text{ mm h}^{-1}$  when nonseeded. Differences in crystal habits in the natural and seeded clouds were similar to those observed in experiments 1 and 2 in terms of both IPC and precipitation rates.

Light precipitation was observed briefly at the Snow Lab prior to 1540, but it did not exceed  $0.2 \text{ mm h}^{-1}$ . This shower preceded the arrival of the seeded zone and is thought to have been of natural origin. Heavier precipitation began at 1601, diminished after 1616, and essentially ceased after 1633. The heavier shower coincided with the passage of the seeded zone, which was over the Snow Lab from 1559 to 1629 (Fig. 11).

The network precipitation amounts coincident with the passage of the third seeding line ranged from 0.025 mm at the West Arm site (near the west end of the seeding arc) to 0.20 and 0.35 mm at the GMO East and West sites, respectively. The upwind Mesa Lakes gage caught 0.125 mm, and the downwind Ward Creek gage caught 0.10 mm, both less than the sites nearer the target. By 1645, precipitation was no longer being recorded by the two gages closest to the Snow Lab.

#### d. Airborne seeding experiment 4

The fourth and final line of AgI generated on 18 Mar was released near 1635 only 9 km upwind of the Snow Lab and within the accelerated flow over the mesa top. Digital satellite imagery indicated cloud tops as cold as  $-18^{\circ}\text{C}$  over the Snow Lab and  $-20^{\circ}\text{C}$  15 km north of it.

On the first sampling pass IPCs in excess of  $200\text{ L}^{-1}$  were found coincident with the AgI, followed by SLW contents farther south of  $0.1\text{--}0.2\text{ g m}^{-3}$ . The following two passes revealed some broadening of the ice particle plume and depletion of the SLW. However, the along-the-wind width of the enhanced IPC zone was less than 5 km as it passed over the Snow Lab. In contrast, widths exceeded 10 km during the first three experiments. The final sampling pass, only 31 minutes after seeding, showed that much of the seeded cloud had already been subjected to the lee side subsidence and had dissipated.

Mean seeded IPCs were  $7\text{ L}^{-1}$  in the 5 km zone upwind of the Snow Lab, compared to  $1\text{ L}^{-1}$  when the zone was nonseeded. Estimated precipitation rates at the 3.8 km level were 0.16 and  $0.04\text{ mm h}^{-1}$  in the seeded and nonseeded zones, respectively. The estimated precipitation rate in the seeded zone was much less than observed in experiment 3, 1.5 h earlier, probably reflecting the short time available for crystal growth after nucleation.

Precipitation at the Snow Lab began at 1700, 12 minutes after the passage of the leading edge of the seeded zone aloft and 4 minutes after the passage of the trailing edge (Fig. 11). Thereafter, natural snow continued at most gage sites for several hours. It is believed that seeding did not cause any significant snowfall during this experiment, because time was inadequate for the growth and fallout of seeding-caused crystals to the Snow Lab.

#### e. Airborne seeding experiment 5

Northerly flow persisted on the morning of 19 Mar, again producing orographic cloud. Clouds tops were at 4.6 km and  $-19^{\circ}\text{C}$ . Mean IPCs were initially  $3\text{--}4\text{ L}^{-1}$ , and cloud base was measured at 3.4 km, about 200 m higher than the previous day. The climbout sounding is shown in Fig. 2c. After about two hours of ground-released seeding (see section 3), it was thought that enough SLW was present to warrant additional aircraft seeding experiments.

The fifth aerial seeding arc (the first of 19 Mar) was generated 23 km upwind of the Snow Lab, again at 3.8 km altitude and  $-13^{\circ}\text{C}$ . Seeding took place near 1356 and was followed by six sampling passes. The somewhat broken orographic cloud deck extended 17 km upwind of the Snow Lab. In contrast to the previous day's sampling, the ground near the lab was sometimes visible from the aircraft.

Ice particle concentrations in the seeded zones ranged from 20 to  $100\text{ L}^{-1}$ , while natural IPCs often

reached  $15\text{ L}^{-1}$ , much higher than those observed on the previous day. Evaluation of the 2D-C images recorded within the 5 km immediately upwind of the Snow Lab revealed a tripling of IPC, from  $1.8\text{ L}^{-1}$  when nonseeded to  $7.2\text{ L}^{-1}$  when seeded, while the seeded precipitation rate was twice the nonseeded. However, the enhanced IPC zone was not very pronounced and was only a few kilometers wide (N-S) prior to and during passage over the Snow Lab. It achieved much greater IPC values and became 5–10 km wide when observed downwind of the Snow Lab. In experiment 2, when AgI was released a similar distance upwind, an enhanced IPC zone over 10 km wide was apparent while passing over the Snow Lab. The much narrower width and later development of high IPCs during experiment 5 may have been due to more limited interaction with SLW in the drier, broken cloud deck of 19 Mar.

No appreciable precipitation was recorded at the Snow Lab until 1453, some 20 minutes too late to have been related to the passage of the seeded zone. The gage network recorded no precipitation throughout the duration of the experiment; consequently, there was no evidence that seeding increased snowfall on the mesa.

#### f. Airborne seeding experiment 6

The sixth and final airborne seeding arc (the second of 19 Mar) was generated near 1454, 28 km upwind of the Snow Lab. Satellite imagery showed the broken cloud deck still extending about 18 km north of the Snow Lab. Cloud top temperatures at the time of seeding were  $-18^{\circ}\text{C}$  over the target and  $-22^{\circ}\text{C}$  some 8 km upwind of it.

On the first of seven sampling passes, the AgI plume was missed, and the (natural) IPC often reached  $7\text{ L}^{-1}$  over the mesa. Increased IPCs ranging from 15 to  $100\text{ L}^{-1}$  were found coincident with AgI on five of the remaining six passes (only AgI was detected on the second pass), while natural IPCs often reached 5–10  $\text{L}^{-1}$  from 5 km north to 10 km south of the Snow Lab. Liquid water was generally encountered only in the few kilometers immediately upwind of the Snow Lab. The N-S extent of the enhanced IPC zone was again limited to a few kilometers while upwind and over the Snow Lab, and maximum IPC was only about  $15\text{ L}^{-1}$  on the two passes with the seeded zone just upwind of or over the Lab.

Mean IPC in the 5 km zone upwind of the Snow Lab was  $2.5\text{ L}^{-1}$  when seeded but  $2.6\text{ L}^{-1}$  when nonseeded. The estimated precipitation rates were also essentially unchanged. Precipitation began at the Snow Lab at 1520, some 15 minutes before the seeded zone began to pass overhead, so it was almost certainly of natural origin. Snowfall continued until 1550. The seeded plume passed over the Snow Lab between 1535 and 1542, and any precipitation that might have re-

sulted from the seeding was indistinguishable from the natural shower. However, in view of the aircraft observations, it seems unlikely that seeding had much effect on surface snowfall.

*g. Summary of airborne seeding experiments*

Results of the six airborne seeding experiments, along with various supporting information, are summarized in Table 2. The mean nonseeded IPCs in the 5 km zone upwind of the Snow Lab were  $\leq 2.6 \text{ L}^{-1}$  in all cases, with a mean value of  $1.5 \text{ L}^{-1}$  for all six experiments. Mean seeded IPCs ranged from 2.5 to  $21.5 \text{ L}^{-1}$  on the two days, with an overall mean near  $9 \text{ L}^{-1}$ . The majority of the IPC increases appeared as small crystals classified as hexagonal and spherical by the processing software, the latter most likely tiny stellar or hexagonal crystals. Most crystals classified as hexagonal were also small, and most probably of the P1a, P1b, and P1c habits (see Magono and Lee 1966). The majority of crystals in the seeded cloud volumes that were classified as irregular were fragments of dendrites or rimed hexagonal crystals.

Five of the six experiments resulted in significant increases in estimated precipitation rates at the 3.8 km aircraft sampling level. The exception was experiment 6, in which the precipitation rate was essentially unchanged. The mean estimated precipitation rate for the 5 km interval immediately upwind of the Snow Lab was  $0.21 \text{ mm h}^{-1}$  for the seeded clouds from all six experiments, but only  $0.05 \text{ mm h}^{-1}$  for the nonseeded clouds, a factor of 4 difference. Caution is again necessary in regard to quantitative interpretation of the estimated precipitation rates (see Part I).

Very little snowfall was recorded at the Snow Lab within 0.5 h preceding or following the passage of the seeded zones aloft in the first three experiments. The greatest surface snowfall rate was  $1.6 \text{ mm h}^{-1}$  in experiment 3, and in all three experiments the peak rate exceeded  $1.0 \text{ mm h}^{-1}$  during passage of the seeded zone overhead. Total integrated snowfall attributed to seeding was 0.22, 0.10 and 0.18 mm for experiments 1, 2 and 3, respectively. Mean precipitation rates ranged from 0.33 to  $0.43 \text{ mm h}^{-1}$  for these experiments. Super et al. (1986) reported a median rate of  $0.7 \text{ mm h}^{-1}$  for a two-winter period on the Grand Mesa. Thus, the rates observed at the Snow Lab in the first three experiments were similar to natural rates during less intense storms.

The failure of experiment 4 to produce snowfall at the ground is thought to be due to the proximity of the seeding arc to the Snow Lab. The neophyte AgI plume was afforded only 10 minutes for nucleation, growth, and fallout to the Snow Lab, some 600 m below the seeding altitude. Even immediate nucleation and diffusional crystal growth at a rate of  $0.1 \text{ mm min}^{-1}$  (Holroyd 1986) could not have produced crystals of sufficient size to result in detectable surface snowfall so quickly.

TABLE 2. Summary of the six airborne seeding experiments conducted over the Grand Mesa on 18–19 Mar 1986. Seeded zones are denoted by "S," and nonseeded zones by "NS." All seeding and aircraft monitoring was at 3.8 km altitude.

Aerial seeding experiment	Seeding times (mst)	Seeding dist. upwind* (km)	Seeding arc length (km)	No. of sampling passes	No. of passes detected	Mean 2D-C ice particle conc. ( $\text{L}^{-1}$ )**		Mean est'd 2D-C precip. rate ( $\text{mm h}^{-1}$ )**		Precip. at Snow Lab		Did SFC precip. coincide with passage of seeded zone	Mean J-W LWC ( $\text{g m}^{-3}$ )**		Mean temp. at 3.8 km ( $^{\circ}\text{C}$ )	Cloud top alt. (km msl)	Cloud top temp. ( $^{\circ}\text{C}$ )	Aircraft wind speed at 3.8 km*** ( $\text{m s}^{-1}$ )
						S	NS	S	NS	Total (mm)	Mean rate ( $\text{mm h}^{-1}$ )		NS	S				
860318																		
1	1048–1057	37	42	10	10	11.6	0.6	0.24	0.01	0.22	0.33	Yes	0.07	0.03	-14.4	4.0	-17	13
2	1247–1252	19	27	6	6	21.5	0.2	0.40	<0.01	0.10	0.43	Yes	0.05	0.05	-14.1	3.9	-15	12
3	1503–1508	28	40	10	9	12.9	2.0	0.34	0.08	0.18	0.33	Yes	0.04	0.04	-13.8	4.6	-18	11
4	1634–1637	9	26	4	3	7.3	1.0	0.16	0.04	0	0	No	0.08	0.04	-13.5	4.6	-18	11
860319																		
5	1354–1358	23	27	6	4	7.2	1.8	0.08	0.04	0	0	No	0.05	0.05	-13.1	4.6	-19	11
6	1448–1457	28	45	7	6	2.5	2.6	0.08	0.09	(0.22)	(0.40)	Uncertain	0.07	0.03	-12.4	4.5	-20	10
Mean All Experiments																		
		24	34	7	6	9.3	1.5	0.21	0.05	—	—	—	0.06	0.04	-13.6	4.4	-18	11

\* Of Snow Lab.  
 \*\* For 5 km zone north of Snow Lab.  
 \*\*\* Averaged over N-S extent of each experiment.

Experiments 5 and 6 on 19 Mar probably did not produce precipitation at the Snow Lab, but continuous cloud deck did not extend as far upwind as on 18 Mar. Further, the mesa top near the Snow Lab was visible from the aircraft on some 19 Mar passes but was not seen on 18 Mar. The more broken cloud deck with somewhat higher bases on 19 Mar apparently provided less in-cloud time for ice crystal growth. This may have been a limiting factor in producing snowfall at the surface. The drying with time of the atmosphere over the mesa below 60 kPa can be seen by contrasting Figs. 2a and 2c.

While on some passes SLW appeared to be inversely correlated with the enhanced IPC resulting from AgI seeding, the natural temporal and spatial variability of SLW over the mesa masked any obvious drying of the cloud due to seeding in most cases. Liquid water in the seeded 5 km zone immediately upwind of the Snow Lab never exceeded that found in the analogous nonseeded zone and overall was about one-third less than the mean in the nonseeded zone (Table 2). This suggests that the AgI seeding reduced, but did not eliminate, the SLW content of the orographic clouds.

## 5. Conclusions

Eight physical cloud seeding experiments were conducted in northerly flow and shallow orographic cloud over the Grand Mesa of Colorado on 18–20 Mar 1986. Two experiments employed ground-released AgI smoke, while the six others used airborne AgI seeding, also with an acetone generator. Natural snowfall was very limited during the experimental periods.

In all eight experiments, the AgI was consistently detected in cloud by the airborne acoustical ice nucleus counter at the 3.8 km sampling altitude. For the ground seeding experiments this required vertical transport of the AgI of at least 1100 m, which confirms the feasibility of targeting some orographic clouds with either airborne or properly sited ground-based generators.

In all eight experiments, marked enhancements in the observed ice particle concentrations were detected coincident with the AgI plumes. Thus, the efficacy of AgI as a nucleating agent was verified in natural clouds at the temperatures observed ( $-8.5$  to  $-14^{\circ}\text{C}$ ). Large numbers of ice crystals smaller than 0.6 mm, either hexagonal plates (at  $-9$  to  $-12^{\circ}\text{C}$ ) or minute dendrites (at  $-13$  to  $-14^{\circ}\text{C}$ ), were recorded within seeded zones at aircraft sampling altitudes in all eight experiments. A fraction of the seeded crystals grew to larger sizes, and the sizes and habits of these crystals were consistent with the prevailing temperature regimes and estimated growth times. Precipitation rates estimated from aircraft 2D-C probe images recorded in the seeded zones exceeded those estimated for the nonseeded zones in seven of the eight experiments.

Significant precipitation coincident with the passage of the seeded zone aloft in the first three (of six) air-

borne experiments was recorded at the Snow Lab, while virtually no precipitation was recorded at other times during that experimental period. Probable reasons for the lack of precipitation at the surface in the final three airborne experiments, as previously discussed, relate to the insufficient residence time of the AgI and resulting crystals in SLW cloud.

Very light snow reached the mesa from the thin seeded clouds in one ground-based experiment, while no other clouds precipitated. No ground level observations were practical during the other ground-based seeding experiment, but it appeared probable that surface snowfall was increased.

All eight physical seeding experiments produced marked microphysical changes due to AgI seeding in shallow orographic cloud. The resulting IPC enhancements in turn produced an increase in estimated precipitation rates at the aircraft sampling level about 500 m above the Grand Mesa in all but one case. Finally, light but significant precipitation was produced at ground level by at least half of the experiments.

While the physical chain of events from seeding to surface snowfall has often been hypothesized, it has seldom been demonstrated. The ground-based seeding experiments provide direct physical evidence that releasing AgI well up the windward slope of a mountain barrier can alter cloud microphysics in a direction that should lead to increased snowfall. Taken together with the results shown in Part II (Super and Heimbach 1988) and in Holroyd et al. (1988) there is reason to be optimistic concerning the potential of seeding some winter orographic clouds with high-altitude ground-based generators.

The airborne experiments demonstrated that aerial seeding can also result in increased snowfall at the surface under some conditions. Further research of this type will be required to better define those conditions that are suitable for seeding.

The approach used in these experiments is believed to have considerable value for future work. Simple orographic clouds are excellent candidates for testing various seeding methods, rates and agents.

*Acknowledgments.* The authors are pleased to acknowledge the significant contributions to this paper made by several persons. Jack McPartland of the Bureau of Reclamation (Bureau) was the aircraft scientist on some of the missions, while the second author flew on the others. Michael Collins of the Bureau maintained the aircraft, and surface sensors and electronics systems. David Davalos of Aero Systems, Inc., skillfully piloted the aircraft. Marty Thorp and William Hauze of North American Weather Consultants (NAWC) operated the ground-based seeding generator and manned the Snow Lab. John Thompson, also of NAWC, operated the airborne seeding generator and aircraft data acquisition system. Much of the analysis software was developed by Ed Holroyd of the Bureau.

Lonnie Sale, of Systems and Applied Sciences Corporation, developed additional software and made many of the computer processing runs. Cynthia Snook of the Bureau greatly facilitated the writing process by typing the several drafts of the manuscript. The helpful suggestions of the reviewers are also gratefully acknowledged.

This work was done as part of the Bureau's Colorado River Augmentation Demonstration Program under the direction of John Lease.

#### REFERENCES

- Cotton, W. R., G. J. Tripoli, R. M. Rauber and E. A. Mulvihill, 1986: Numerical simulation of the effects of varying ice crystal nucleation rates and aggregation processes on orographic snowfall. *J. Climate Appl. Meteor.*, **25**, 1658-1680.
- DeMott, P. J., W. G. Finnegan and L. O. Grant, 1983: An application to chemical kinetic theory and methodology to characterize the ice nucleating properties of aerosols used for weather modification. *J. Climate Appl. Meteor.*, **22**, 1190-1203.
- Holroyd, E. W., III, 1986: A determination of snow particle nucleation and growth rates in orographic clouds over the Grand Mesa, Colorado. Preprints, 23rd Conf. on Radar Meteorology and Cloud Physics, Snowmass, Amer. Meteor. Soc., J223-J226.
- , 1987: Some techniques and uses of 2D-C habit classification software for snow particles. *J. Atmos. Ocean. Tech.*, **4**, 498-511.
- , J. T. McPartland and A. B. Super, 1988: Observations of silver iodide plumes over the Grand Mesa of Colorado. *J. Appl. Meteor.*, **27**, 1125-1144.
- Magono, C., and C. W. Lee, 1966: A classification system for ice crystal habits. *J. Fac. Sci. Hokkaido Univ.*, Sec. 7, 3, p. 27.
- Super, A. B., and J. A. Heimbach, Jr., 1988: Microphysical effects of wintertime cloud seeding with silver iodide over the Rocky Mountains. Part II: Observations over the Bridger Range, Montana. *J. Appl. Meteor.*, **27**, 1152-1165.
- , E. W. Holroyd III, B. A. Boe and J. T. McPartland, 1986: Colorado River Augmentation Demonstration Program Technical Report: January 1983-March 1985. U.S. Bureau of Reclamation, Division of Atmospheric Resources Research, Denver, CO, May, 1986. 42 p.
- , B. A. Boe, E. W. Holroyd III and J. A. Heimbach, Jr., 1988: Microphysical effects of wintertime cloud seeding with silver iodide over the Rocky Mountains. Part I: Experimental Design and Instrumentation. *J. Appl. Meteor.*, **27**, 1142-1152.